Calculated properties of solid O_2 under pressure at low temperature

R. D. Etters, K. Kobashi, and J. Belak
Department of Physics, Colorado State University, Fort Collins, Colorado 80523
(Received 14 January 1985)

The zero-temperature properties of solid O_2 are calculated at pressures $0 \leq P \leq 70$ kbar by minimizing the Gibbs free energy at each pressure and then using the equilibrium lattice parameters in a harmonic-lattice-dynamics calculation of the dynamical properties. The minimization is based upon a continuously deformable monoclinic unit cell where the internal energy is composed of the static lattice energy and the properly weighted Einstein zero-point energies of the phonon, libron, and vibron modes. The lattice parameters, binding energy, compressibility, pressure-volume relation, libron, phonon, and vibron frequencies, phonon velocities, and dispersion curves are determined at each pressure. The lattice parameters and the phonon, libron, and vibron frequencies show clear evidence of a monoclinic to orthorhombic *Fmmm* structural phase transition at 24 ± 1 kbar. A change in slope of these quantities is also observed at $P \simeq 7$ kbar. A detailed comparison of these results with recent Raman scattering measurements is given.

I. INTRODUCTION

A previous calculation[1] on the high-pressure properties of solid oxygen at low temperatures predicted a monoclinic to orthorhombic phase transition at approximately 6 kbar that was driven by a shear force along the a axis of the crystal, as shown in Fig. 1. This shear results from a partial cancellation of the repulsive van der Waals potential with the attractive magnetic interaction. Also calculated were the pressure dependence of the libron and vibron frequencies, the phonon velocities, the equilibrium lattice parameters, and the pressure-volume curve. Subsequently, low-temperature Raman measurements were made to 60 kbar by Meier, van Albada, and Lagendijk[2] (MvAL) that showed abrupt changes in the slope of the vibron and libron frequencies at $P=11\pm3$ and 8 ± 1 kbar, respectively. Concurrently, Jodl *et al.*[3] observed the same behavior at approximately 4 kbar. This was interpreted as a phase transition and the Raman spectra are entirely consistent with predicted transition at 6 kbar. The measurements of Jodl *et al.* also showed an abrupt change in slope of both the libron and vibron frequencies at about 28 ± 2 kbar, which was not detected in the MvAL experiment[2] or in the theory.[1] These and other zero-pressure measurements of Cahill and Leroi[4] at low-temperature show Raman peaks at 43 ± 1 and 79 ± 2 cm^{-1}, which are interpreted as libron modes.

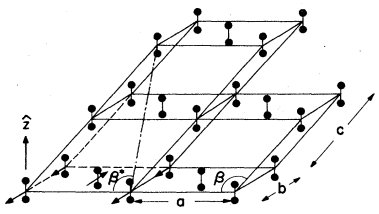

FIG. 1. Monoclinic unit cell of α-O_2. Lattice parameters are the lengths a,b,c, and the angle β. At $\beta^*=90°$, this lattice becomes the orthorhombic *Fmmm* structure. Arrows designate the directions of the magnetic moments.

In the previous calculation,[1] the libron and vibron frequencies showed no evidence of an abrupt change in slope at the transition. Instead the transition was identified by a dramatic decrease in one of the transverse acoustic shear mode velocities at pressure $P \simeq 6$ kbar and by the lattice parameters which clearly showed a monoclinic to orthorhombic structural transition. Otherwise, the pressure dependence of the vibron and libron frequencies were in reasonably good agreement with experiment. In this previous publication,[1] however, the important cubic intramolecular potential term was inadvertently omitted from the dynamical matrix and the reported vibron frequencies are all too low. This correction has been made and reported in an erratum.[1] Another prediction was that the two librons at zero pressure have zone-center frequencies of 46 and 52 cm^{-1}, respectively. All other previous calculations[5] have yielded approximately the same result, where the splitting between the modes was either slightly less or slightly greater depending on the potential used. In no previous calculation has the observed high-frequency libron peak at 79 cm^{-1} been predicted and various explanations for this apparent failure of the theory have been put forward.[5] A recent conjecture[6] is that the magnetic unit cell, which contains two molecules, is the appropriate cell for interpreting the Raman data, rather than the traditional one-molecule crystallographic unit cell.[7] Supporting this conjecture is that a zone-center libron with frequency near the observed[2-4] zero-pressure Raman peak at 79 cm^{-1} is an expected prediction. However, interpretation of the dynamical data on the basis of either unit cell presents problems that presently cannot be resolved, over which there is considerable controversy. In this work these problems are somewhat circumvented by presenting results based upon both descriptions and a detailed discussion of their relative merits and liabilities is presented in Sec. IV.

Until now there has been little high-pressure experimen-

tal data upon which comparisons with theory could be made. However, the recent Raman measurements[2,3] provide results which, while in reasonable qualitative agreement with the previous theory,[1] contain features that were not predicted. The objective of this work is to refine the accuracy of the calculations and focus attention at those pressures where phase transitions and other distinct features manifest themselves so that a more detailed understanding of the properties of solid O_2 under pressure and their relationship to the experimental observations is exposed.

II. THEORY

The van der Waals potential between two O_2 molecules (i,j) is given in terms of a site-site expression

$$U_V(i,j)=\sum_{s=1}^{4}\{Ae^{-\alpha r_s}-f(r_s)[(B_6/r_s^6)+(B_8/r_s^8)+(B_{10}/r_s^{10})]\}+U_{\rm EQQ}\ , \tag{1}$$

where $A=1.944\,114\times10^7$ K, $\alpha=3.8$ Å^{-1}, $B_6=0.150\,769\,4\times10^6$ K Å^6, $B_8=-0.696\,602\,1\times10^6$ K Å^8, and $B_{10}=0.956\,239\,1\times10^7$ K Å^{10}. The sum over s extends over the four distances between the two interaction sites on each molecule, placed at the atomic positions which are 1.208 Å apart at $P=0$. The long-range dispersion terms are damped by the standard factor[8]

$$f(r_s)=\begin{cases}\exp\{-[(1.28r_m/r_s)-1]^2\}, & r_s\le 1.28r_m\\ 1, & r_s>1.28r_m\end{cases} \tag{2}$$

where $r_m=3.3$ Å. The coefficients B_6, B_8, and B_{10} are determined so that the well and long-range part of the potential agrees with a previous expression[1] that was found to give good agreement with experiment for the second virial coefficients and the zero-pressure structural properties[7] of α-O_2. The parameters A and α were chosen to be within the range of uncertainty of expressions deduced from molecular beam scattering and recent *ab initio* data. The weak electric quadrupole-quadrupole interaction $U_{\rm EQQ}$ was described by placing point charges $(-q,2q,-q)$ along the molecular axis at (0.6038,0,−0.6038 Å), respectively, with respect to the mass center so that the observed quadrupole moment $Q=-0.39\times10^{-26}$ esu cm^2 is reproduced. The potential $U_{\rm EQQ}$ between two molecules is then given by the Coulomb interaction between the charges on the two different molecules.

It is now well known[9] that the antiferromagnetic Heisenberg interaction

$$U_M(i,j)=2\sum_{\substack{i,j\\ i<j}}J(R_{ij})\hat{\mathbf{S}}_i\cdot\hat{\mathbf{S}}_j \tag{3}$$

is an essential component in the description of the O_2 pair potential and is responsible for stabilizing the α phase over the β phase at low temperature and pressure. In Eq. (3), R_{ij} is the distance between mass centers of molecules (i,j) and the $\hat{\mathbf{S}}_i$ are unit vectors that define the direction of the magnetic moments. In this and previous work[1,9] these unit vectors are constrained to be along the b axis of the crystallographic cell in the antiferromagnetic order as established by experiment.[10] As a consequence, the small anisotropic terms[11] in the magnetic interaction that establish the direction of the moments with respect to the crystal axes can be replaced by this constraint and otherwise ignored. The exchange energy J is taken to be

$$J(R)=J_0\exp[-\alpha(R-R_0)+\beta(R-R_0)^2]\ , \tag{4}$$

where $J_0=30$ K is the value of the exchange energy at the calculated nearest-neighbor separation $R_0=3.1854$ Å at pressure $P=0$, and $(\alpha,\beta)=(3.5$ Å$^{-1},1.2$ Å$^{-2})$, respectively. Recent neutron scattering[12] and magnetic susceptibility data[13] give $25\le J_0\le 38$ K. It is clear from the form of Eq. (4) that the exchange energy is represented as a function of only the distance between mass centers R, whereas *ab initio* results[14] indicate that there is a strong dependence on the relative orientation between molecules. Fortunately, for the crystal structures found in this work the molecular axes are collinear and the magnetic interaction between molecules in the a-b plane of the crystal totally dominates contributions from out-of-plane molecules. Thus, only magnetic interactions between parallel molecules need be considered, for which Eq. (4) provides a totally adequate description. The quadratic term in Eq. (4) was introduced in order to accurately reproduce the observed $P=0$ lattice structure.[7] This high level of agreement could not otherwise be achieved. For $R<2.6$ Å, $P\gtrsim 50$ kbar, the parameters in Eq. (4) are given by $J_0=19.885$ K, $\alpha=4.9$ Å, $\beta=0$, which are determined by ensuring that $J(R)$ and its first derivative are continuous at $R=2.6$ Å. Experimental data for $J(R)$ exists[13] only up to pressures $P=6$ kbar, which corresponds to a nearest-neighbor distance of $R=3.03$ Å. A comparison of $J(R)$ with experimental results,[12,13] *ab initio* data for a pair of isolated molecules,[14] and the expression used in previous work,[1] shows that it is clearly within the range of existing uncertainty.

Finally, the intramolecular interaction between oxygen atoms in the O_2 molecule is given by

$$U_{\rm intra}\simeq\tfrac{1}{2}k(d-d_0)^2+g(d-d_0)^3\ , \tag{5}$$

where the force constants k and g and the equilibrium bond length d_0 are taken from gas-phase spectroscopic data given in Herzberg.[15] Thus the total potential is

$$U_T=\sum_{\substack{i,j=1\\ i<j}}^{N}[U_V(i,j)+U_M(i,j)]+\sum_{i=1}^{N}U_{\rm intra}(i)\ . \tag{6}$$

The results were obtained as follows. A pattern-search optimization of the Gibbs free energy

$$G=U_T+E_{\rm ZP}+PV \tag{7}$$

was initiated at each pressure with the lattice parameters (a,b,c,β) and the bond length d taken as independent variables. Lattice sums were taken that include the 280

nearest neighbors, which is an interaction range of about 15 Å. In Eq. (7) V is the molar volume and E_{ZP} is the zero-point energy evaluated by calculating all the Einstein frequencies of the phonons, librons, and internal vibrations (vibrons) at each stage in the optimization. To test the accuracy of the zero-point energy calculation, E_{ZP} was also calculated at $P=0$, 20, and 50 kbar by averaging the lattice-dynamical frequencies over the Brillouin zone of the crystal and the results were consistently about 9% lower than from the Einstein determination. Thus, in the pattern-search minimization, the Einstein zero-point energies were scaled by a factor $f=0.912$ to improve the quality of the structural determination, even though this difference is a small effect. Thus

$$E_{ZP}=\frac{f}{2}\sum_{i,\alpha}\hbar\omega_{i\alpha}\,, \tag{8}$$

where i sums over each molecule in the unit cell and $\alpha=1,2,\ldots,6$, is a sum over all independent modes of oscillation with Einsten frequencies $\omega_{i\alpha}$.

The lattice parameters and bond lengths determined by the above-mentioned minimization are then introduced into a lattice-dynamics calculation and d and the orientation of the molecules are further refined by minimizing the Gibbs free energy with respect to them at each pressure. Lattice sums are taken out to 280 neighbors as before, except for the magnetic interaction where only the first two nearest-neighbor shells are important. Details of the pattern-search optimization and the lattice dynamics are given elsewhere.[1,9] Out-of-plane contributions to the magnetic interaction were calculated using the orientational-dependent expression for J derived from *ab initio* data.[14] As mentioned above, these contributions were found to be negligible. The minimization of the energy with respect to the orientation of the molecular axes of each molecule in the unit cell showed they are collinear and point normal to the a-b plane.

III. RESULTS

The second virial coefficients were determined from U_T, given by Eq. (6), and the results were found to be in good agreement with experiment.[16] In that calculation the average of the magnetic interaction $\langle\sum_{i<j}U_M(i,j)\rangle$ was taken to be zero as is appropriate for a paramagnetic gas. The calculated lattice parameters, molar volume V, and binding energy E, determined at $P=0$, are shown in Table I. These values for (a,b,c,β,V,E) are in close agreement with the experimental values (5.375 Å, 3.42 Å, 5.065 Å, 132.18°, 20.81 cm^3/mole, 1042 K).[7,17] The calculated nearest-neighbor distance is 3.1854 Å compared to the experimental value[7] of 3.186 Å. The calculated bond length is $d=1.20719$ Å. The binding energy is $E=U_{stat}$

TABLE I. The values of the lattice parameters (a,b,c,β,β^*) and the intramolecular bond length d that minimize the Gibbs free energy vs pressure. Calculated volumes and energies are also displayed.

V (cm^3/mole)	P (kbar)	a (Å)	b (Å)	c (Å)	β (deg)	β^* (deg)	d (Å)	E (K)
20.88	0	5.355	3.448	5.058	132.04	100.70	1.207 19	−1056
19.57	2.5	5.212	3.377	4.940	131.62	100.35	1.207 00	−1040
18.68	5.0	5.103	3.331	4.849	131.18	99.97	1.206 83	−1001
18.27	6.5	5.049	3.310	4.798	130.84	99.59	1.206 74	−974
17.91	8.0	5.003	3.291	4.761	130.64	99.42	1.206 62	−943
17.69	9.0	4.966	3.285	4.725	130.33	99.08	1.206 61	−920
17.47	10.0	4.944	3.267	4.700	130.17	98.86	1.206 54	−892
17.30	11.0	4.914	3.263	4.682	130.06	98.82	1.206 50	−874
17.12	12.0	4.888	3.254	4.658	129.88	98.62	1.206 45	−849
16.96	13.0	4.863	3.247	4.639	129.75	98.52	1.206 40	−825
16.80	14.0	4.835	3.243	4.610	129.46	98.20	1.206 36	−799
16.64	15.0	4.810	3.236	4.589	129.31	98.05	1.206 31	−773
16.51	16.0	4.788	3.230	4.570	129.15	97.89	1.206 26	−747
16.37	17.0	4.762	3.227	4.543	128.88	97.58	1.206 21	−719
16.23	18.0	4.731	3.228	4.510	128.51	97.15	1.206 17	−691
15.99	20.0	4.686	3.221	4.467	128.06	96.66	1.206 10	−634
15.77	22.0	4.647	3.214	4.429	127.68	96.25	1.206 01	−579
15.70	22.5	4.620	3.224	4.391	127.14	95.57	1.206 00	−561
15.61	23.0	4.528	3.290	4.179	123.63	90.83	1.206 00	−537
15.50	24.0	4.508	3.287	4.143	123.02	90.06	1.205 96	−505
15.31	26.0	4.479	3.277	4.133	123.04	90.23	1.205 89	−448
15.12	28.0	4.448	3.268	4.111	122.78	90.03	1.205 82	−387
14.94	30.0	4.408	3.268	4.091	122.63	90.03	1.205 76	−324
14.55	35.0	4.345	3.244	4.062	122.44	90.10	1.205 60	−171
14.19	40.0	4.276	3.230	4.028	122.09	90.02	1.205 48	−7.61
13.84	45.0	4.216	3.206	4.004	121.87	90.01	1.205 43	169
13.52	50.0	4.148	3.191	3.976	121.44	90.00	1.205 31	357
13.31	55.0	4.113	3.181	3.956	121.35	90.02	1.205 16	491
12.67	70.0	4.012	3.137	3.899	120.96	90.00	1.204 71	991

$+U_{ZP}(l,p)$ where $U_{stat}=\sum_{i<j}(U_V+U_M)$ and $U_{ZP}(l,p)$ is the libron and phonon contributions to the zero-point energy. The term involving U_{intra} in Eq. (6) and the vibron contribution to the zero-point energy $E_{ZP}(v)$ are interpreted as internal self-energies of the molecules. The solid line in Fig. 2 is the calculated pressure-volume (P-V) relation at temperature $T=0$, and the circles represent the experimental data of Stevenson[18] at $T=16$ K, where the reference volume at zero pressure[7] is $V_0=20.8$ cm^3/mole. This data and the points represented by the square[19] and triangle[7] were taken at temperatures sufficiently low that a direct comparison with our calculation can be made without introducing thermal corrections. The experimental data of Stevenson at $T=33$ K, not shown in Fig. 2, can also be compared with our zero-temperature results by taking into account the measured α-β transition volume change and thermal expansion.[7] A comparison of all the above data with our calculated P-V curve is very good. The diamonds represent the experimental data of Stewart[20] at $T=51$ K, but no attempt was made to compare with our $T=0$ results because α-β and β-γ transition volume changes and thermal expansion cannot be accurately determined, except near $P=0$, where such corrections give good agreement with our results. The calculated isothermal compressibility at $T=0$ K and low pressure is $K=(2.99\pm0.3)\times10^{-11}$ cm^2/dyn compared to the experimental value[7] extrapolated to 0 K of $K_{expt}=2.76\times10^{-11}$ cm^2/dyn.

The calculated lattice parameters versus pressure are shown in Fig. 3. Parameters (a,b,c) are identified by the circles, triangles, and squares, respectively. The solid inverted triangles represent experimental data[7] extrapolated to zero temperature and the solid diamonds show experimental data[19] taken at $T=19.1$ K. Two features are important in these curves. First, the slope of the lattice parameters a and c changes rather abruptly at $P\simeq7$ kbar. The slope of the lattice parameter b also changes considerably in this region but it seems to be more continuous in nature. Additional data points at low pressure, not shown here, confirm this behavior. As will become more obvious later, this change in slope does not appear to be associated with a phase transition but this feature does appear in other physical properties and may be associated with some as yet unidentified instability. Secondly, abrupt changes in the values of the lattice parameters occur at $P\simeq23$ kbar, which is clearly identified as a transition from the monoclinic α-phase structure to an orthorhombic $Fmmm$ structure, which is known to be stable near room temperature at higher pressures.[21] The solid lines are intended only to aid the eye. Figure 4 shows the pressure depen-

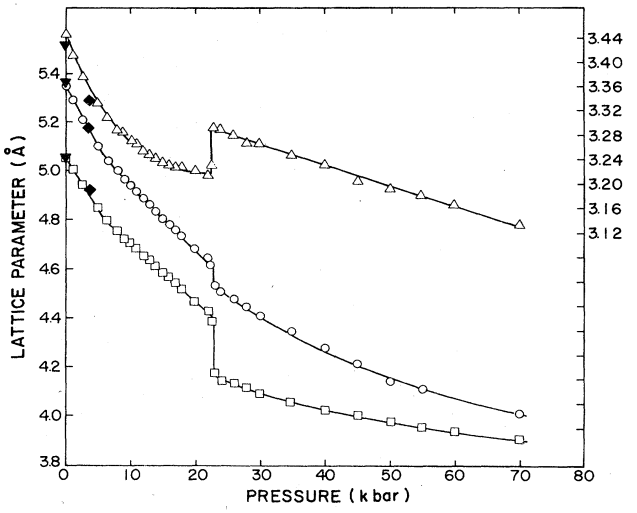

FIG. 3. Squares, circles, and triangles, connected by solid lines, are the calculated lattice parameters c, a, and b vs pressure, respectively. Lattice parameters b refer to the right-hand scale. Solid diamonds[19] and inverted triangles (Ref. 7) show low-temperature experimental data.

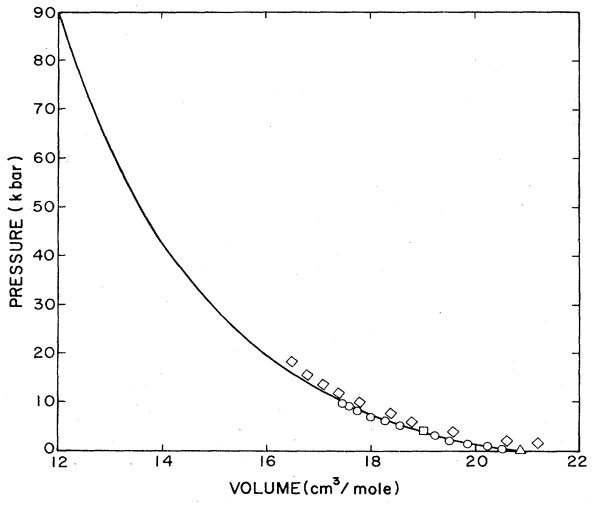

FIG. 2. Solid line gives the calculated zero-temperature P-V curve. Circles (Ref. 18), square (Ref. 19), and triangle (Ref. 7) represent experimental results at low temperature and the diamonds are experimental results (Ref. 20) at $T=51$ K.

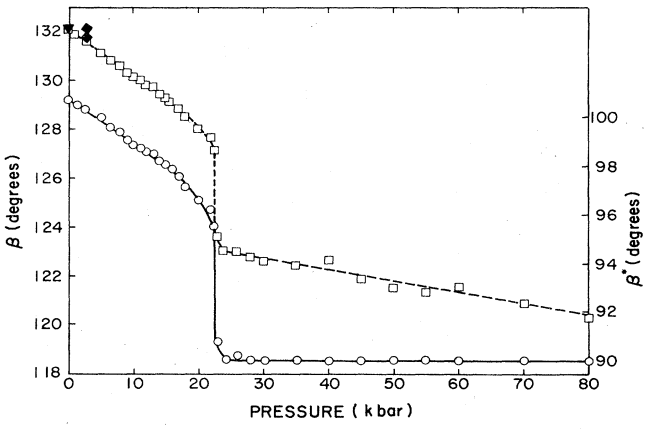

FIG. 4. Squares connected by the dashed line are the calculated angle β vs pressure (left-hand scale) and the solid diamonds (Ref. 19) and inverted triangle (Ref. 7) show low-temperature experimental data. Circles connected by the solid line (right-hand scale) show the calculated angles β^*.

dence of the calculated angles β and β^*, given by squares connected by the dashed line and circles, connected by the solid line, respectively. The solid diamonds[19] and inverted triangles[7] show the low-temperature experimental data. These angles are identified in Fig. 1. It is noted that these angles do not show any change in slope near $P=7$ kbar, as do the other lattice parameters, but do show an abrupt change at the orthorhombic transition pressure. It is also noted that $\beta^*=90°$ for all $P>24$ kbar, characteristic of the orthorhombic structure. By comparing the volume $V=abc\sin\beta$, determined from the lattice parameters on both sides of the orthorhombic transition, an upper limit of $\Delta V=0.05$ cm^3/mole is assigned to the transition volume change.

The change in vibron frequencies in the solid, $\Delta\nu=\nu(P)-\nu(0)$, are shown on Fig. 5. Because of the controversy surrounding the proper description of the unit cell, the results based upon both the crystallographic and the magnetic unit cell are presented. The squares are the calculated frequencies for the vibron associated with the one-molecule crystallographic unit cell. The circles[2] and triangles[3] are selected data points from recent Raman measurements. The calculations show reasonably abrupt changes in slope at $P\simeq7.5$ and 28 kbar, which we identify with the changes in lattice parameters shown in Figs. 3 and 4. This is consistent with the Raman data of Jodl *et al.*[3] (triangles), where sharp changes in slope of the vibron frequency at $P\simeq4$ and 28 ± 2 kbar are reported. The Raman data of MvAL (Ref. 2) (circles) shows a sharp change in slope at $P\simeq12$ kbar but there is no indication of a similar change at higher pressures. These changes in slope from the Raman experiments[2,3] cannot be easily seen from the selected data points displayed in Fig. 5 but they are quite evident from the original results. Based upon the magnetic unit cell, which contains two molecules, another vibron mode is expected and the calculated results for that mode are given by the diamonds. This mode corresponds to the two molecules vibrating out of phase and normally would be expected to have low intensity in Raman scattering, as seems to be the case since it is not observed experimentally. The solid and dashed lines are approximate linear fits to the calculated data points. Because of the difficulty in detecting the finer details in Fig. 5, an expansion of the low-pressure vibron data is presented in Fig. 6, where the solid circles are the calculated data points. While it is not possible to assert that there is a discontinuous change in $d\nu/dP$, it is clear that the slope does change from one constant value to another in the vicinity of $P\simeq7.5$ kbar. Allowing for the calculational uncertainty, which is slightly less than the dimension of the solid circles, the data could be reasonably well fit by two intersecting straight lines with different slopes, as shown by the solid curve.

The two calculated libron frequencies based upon the crystallographic unit cell are shown in Fig. 7 by the lowest-frequency curve of solid circles and the triangles. At $P=0$ these modes, which are characterized by librations about the a and b axes, are nearly degenerate with frequencies of approximately 40 cm^{-1}. With increasing pressure a change in the slope of these frequencies occurs at $P\simeq6$ kbar, and above about 12 kbar they split apart with the libration L_b about the b axis being higher. At approximately 23 kbar there is an abrupt change in L_b and a smaller one in L_a, signaling the orthorhombic phase transition. The only low-frequency libron observed from Raman data is given by the solid line (Jodl *et al.*)[3] and the dashed line (MvAL).[2] The MvAL and Jodl *et al.* data give considerably different values at low pressures but show changes in slope of the libron frequency at about 8 and 4 kbar, respectively. The Jodl *et al.* data also show another change in slope at $P\simeq28$ kbar, which is not observed in the MvAL data. Above 24 kbar, the calculated

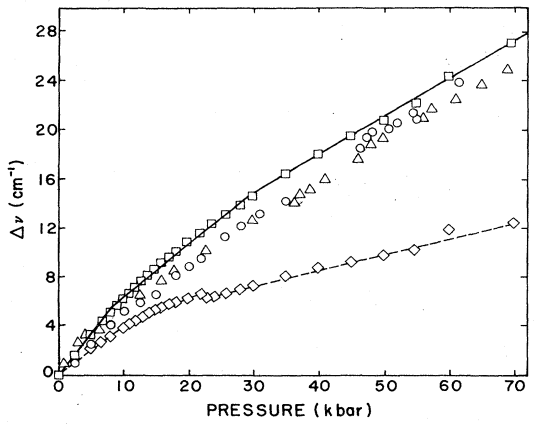

FIG. 5. Squares connected by the solid line give the calculated shifts in the vibron frequency vs pressure based upon the crystalographic unit cell. Circles (Ref. 2) and triangles (Ref. 3) represent low-temperature Raman spectroscopic results. In addition to the high-frequency branch (squares) the magnetic unit cell predicts another branch, given by the diamonds connected by the dashed line.

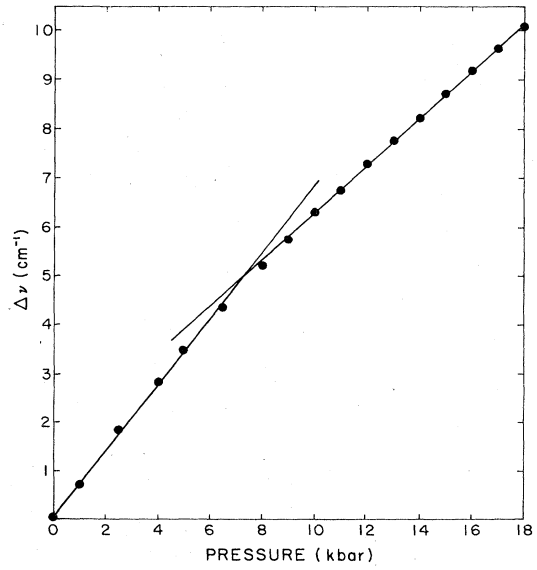

FIG. 6. Solid circles give the calculated shift in the vibron frequency vs pressure, based upon the crystallographic unit cell. Solid lines are approximate fits through the data.

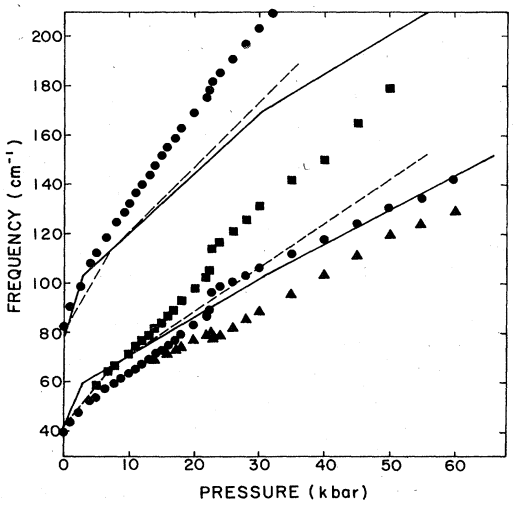

FIG. 7. The low-frequency branch of solid circles and triangles give the calculated L_b and L_a libron frequencies, respectively, vs pressure, based upon the crystallographic unit cell. Dashed (Ref. 2) and solid (Ref. 3) lines show the originators fit to their experimentally Raman data. In addition, the magnetic unit cell predicts two additional libron modes given by the upper branch of solid cirlces and the squares. Dashed (Ref. 2) and solid (Ref. 3) lines near the uppermost branch are the experimental data.

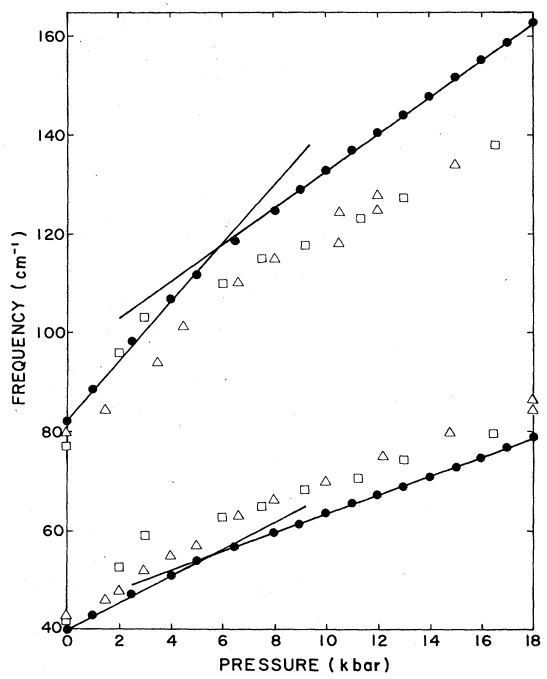

FIG. 8. Diamonds (Ref. 2) and squares (Ref. 3) are the observed libron frequencies and the solid circles are the calculations. Solid lines are approximate fits through the calculated data.

L_b libron frequency is in good agreement with the Jodl *et al.* data, whereas the MvAL data are at somewhat higher frequencies.

Based upon the magnetic unit cell, two additional librons are predicted corresponding to out-of-phase librations of the two molecules in the unit cell about the a and b axes. These modes are represented by the high-frequency curve of solid circles and the squares in Fig. 7. At zero pressure our calculation gives a high-frequency libron at about 81 cm^{-1} and a change in slope occurs at $P \simeq 6$ kbar. At $P \simeq 23$ kbar, the frequency shows a small nearly discontinuous change and then monotonically increases with a different slope at higher pressures. This is qualitatively the same as the Jodl *et al.* (solid line), which gives the first slope change at $P \simeq 4$ kbar and the second at $P \simeq 28$ kbar but, as for the other modes, there is no indication of a change in the MvAL data (dashed line) near the proposed orthorhombic transition pressure. The quantitative agreement with experiment is good up to 10 kbar but, at higher pressures, the calculated frequencies are on the order of 15% too high. The other out-of-phase mode predicted on the basis of the magnetic unit cell lies between the two in phase modes and the high-frequency out-of-phase mode, and is identified by the squares. It is not observed experimentally. It must be noted that the solid and dashed lines are the previous author's[2,3] fit to their experimental data, which are either too sparse or with sufficient experimental uncertainty or both to clearly indicate whether or not the slope changes are discontinuous as shown, or are more gradual over a range of several kbar. The solid circles in Fig. 8 show an enlargement of the two calculated librational modes over the pressure

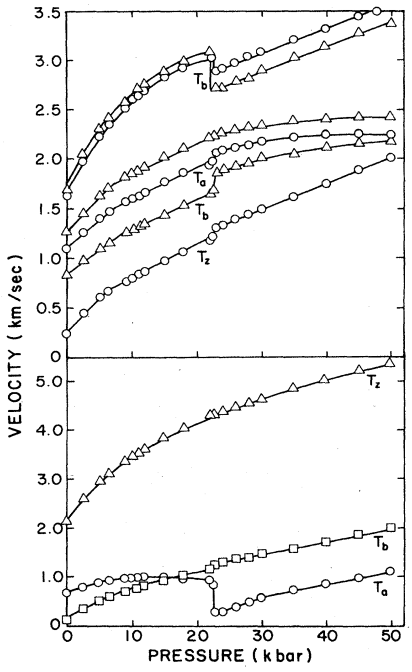

FIG. 9. Circles and triangles connected by solid lines on the upper graph show the calculated phonon velocities vs pressure for modes propagating with wave vector **k** perpendicular to the a-c and b-c planes, respectively. Triangles, circles, and squares connected by solid lines on the lower graph show phonon velocities propagating with **k** perpendicular to the a-b plane.

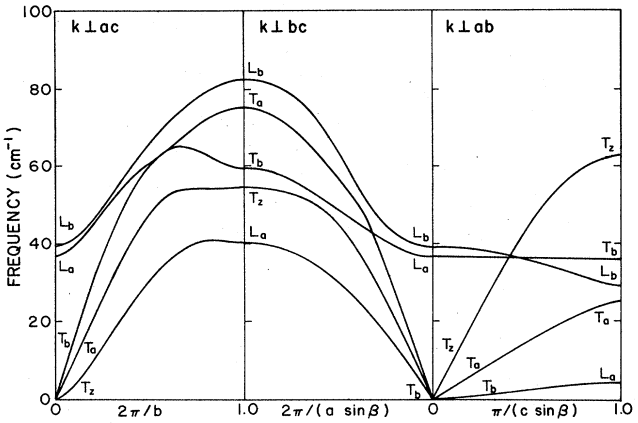

FIG. 10. Dispersion curve at $P=0$ based upon crystallographic unit cell.

range $0 \leq P \leq 18$ kbar that presumably correspond to those observed.[2,3] For both modes the results can be very accurately fit to two straight lines (solid lines) which intersect at about 6 kbar. The change in slope seems quite abrupt at this point but one cannot rule out a more gradual change in dv/dP over an approximately 2-kbar interval.

Figure 9 shows the acoustic phonon velocities versus pressure propagating along different directions **k**. The circles on the top graph show velocities with **k**$\perp ac$ plane, and the assignments T_a, T_b, and T_z refer to the crystallographic axis about which the molecules oscillate. The triangles represent modes with **k**$\perp bc$. On the bottom graph the phonon velocities for **k**$\perp ab$ plane are displayed. As with the other properties, nearly all the phonon modes show an abrupt change in velocity at $P \simeq 23$ kbar, associated with the orthorhombic transition. In fact, the transverse acoustic shear mode T_a, with **k**$\perp ab$, nearly goes to zero at the transition. Also, some of the velocities show a significant change in slope at $P \simeq 7$ kbar. Figures 10 and 11 show the dispersion curves at $P=0$, based upon the crystallographic and the magnetic unit cells, respectively.

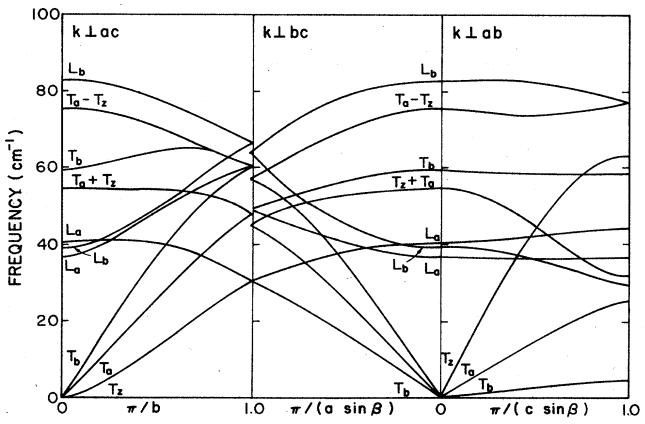

FIG. 11. Dispersion curve at $P=0$ based upon the magnetic unit cell.

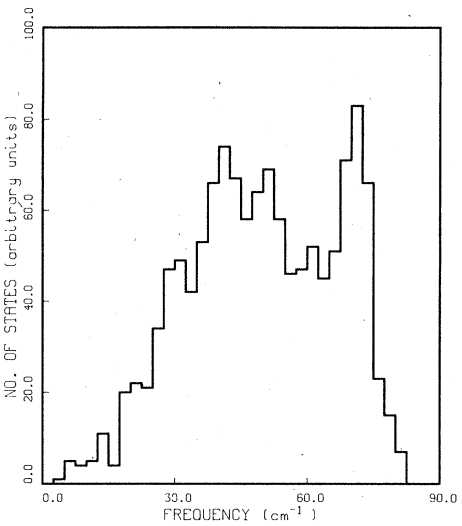

FIG. 12. Calculated density of states at $P=0$ for the magnetic unit cell.

For the magnetic cell, the upper branches of L_a and L_b correspond to librations about these two axes with each of the two molecules librating out of phase. Figure 12 shows the density of states at $P=0$ based on the magnetic unit cell.

The rms librational amplitudes are calculated using the in-phase zone-center librational frequencies L_a and L_b. That is, $\langle \theta_i^2 \rangle \simeq \hbar/2IL_i$, $i=a,b$, where I is the moment of inertia of the molecule. At $P=0$, $\langle \theta_a^2 \rangle^{1/2}$ and $\langle \theta_b^2 \rangle^{1/2}$ are approximately 10.9°.

IV. DISCUSSION AND CONCLUSIONS

The major accomplishments of this work are as follows.

(a) The calculated second virial coefficients are in good agreement with experiment.[16]

(b) The predicted low-energy lattice at $P,T=0$ is the observed $C2/m$, α structure.[7,10] The calculated lattice parameters (a,b,c,β) are in nearly exact agreement with experiment,[7] the largest difference being 0.7%. The molar volume,[7] sublimation energy,[17] and compressibility[7] also agree closely with experiment.

(c) The P-V curve is in good agreement with experiment,[18–20] see Fig. 2.

(d) The pressure dependence of the vibron frequency is in good agreement with experiment[2,3] over the entire pressure range $0 \leq P \leq 70$ kbar.

(e) The pressure dependence of the low-frequency libron L_b is in good agreement with experiment[2,3] at all pressures and, based upon the magnetic unit cell, a high-frequency libron with frequency 81 cm^{-1} at $P=0$ is predicted that may be the mode observed in Raman[2–4] scattering measurements but heretofore not predicted by theory.

(f) The predicted structural and dynamic properties give clear evidence of a weakly first-order monoclinic to orthorhombic phase transition at $P=24\pm1$ kbar, which is

consistent with the Jodl *et al.*[3] Raman experimental observations of a phase change at $P=28\pm2$ kbar. This transition is driven by a shear force along the a axis of the crystal that results in a softening of the transverse acoustic shear mode propagating in the $\hat{\mathbf{z}}$ direction, as shown by Fig. 9, and by an equally dramatic change in the angle β^* from its value appropriate to α-O_2 at $P=0$, to 90° for $P\gtrsim24$ kbar, which characterizes the orthorhombic phase.

(g) The libron and vibron frequencies and some of the lattice parameters and phonon velocities show a distinct change in slope at $P\simeq7\pm1$ kbar, but analysis of the results gives no evidence that this is associated with a phase transition. This is consistent with the phase diagram mapped out by Olinger *et al.*[22] where only the orthorhombic *Fmmm* phase has yet been confirmed from x-ray data in the pressure region above the α phase and below the ϵ phase. A careful examination of the low-pressure Raman data[2,3] shows that it is not possible to resolve dv/dP sufficiently to be assured that it is discontinuous at any pressure, despite the straight-line fits to the data that have been reported. This is because of a divergence in the frequencies reported at each pressure from two different experiments, the inherent error in the measurements, and in some cases due to a paucity of data in the region of the slope change. Thus, in this regard, theory and experiment are consistent with one another.

There remains several unresolved features of solid O_2 under pressure at low temperatures. They are as follows.

(a) Why do the two recent Raman experiments[2,3] show quantitative and qualitative features in the pressure dependence of the libron and vibron frequencies that are sufficiently different to be outside their relative error? In particular, why do only the Jodl *et al.* measurements indicate a phase transition at $P=28\pm2$ kbar when both experiments were nearly identical?

(b) The magnetic unit cell supports one additional vibron and two additional libron modes, as compared to the crystallographic cell. These three modes all are characterized by out-of-phase oscillations of the two molecules in the unit cell. It would therefore be expected that these modes have appreciable Raman intensities only if the spin-orbit coupling significantly enhances the corresponding Raman cross sections. The features of such a mechanism have not been established. Even so, it would then be necessary to explain why the out-of-phase vibron and the in- and out-of-phase libron modes, corresponding to oscillations about the a axis, are not observed. Problems also exist for the predictions based upon the crystallographic unit cell where there seems to be no reasonable potential that will give a single libron mode anywhere near the $P=0$ Raman peak observed at 79 cm^{-1}. Instead, two modes with nearly the same frequencies (~40 cm^{-1}) have been predicted by every calculation to date,[5] including this one. Consequently, the observed peak at 79 cm^{-1} has been attributed by some as an overtone, a two libron peak, or a mixed libron-magnon mode. Then, the observation of only one low-frequency libron instead of two has been explained[5] to be a consequence of the near-degeneracy of these two modes which makes them separately unresolvable. However, recent Raman results[2,3] resolve only one low-frequency libron at all pressures $0\leq P\leq70$ kbar. Thus the above argument holds only if this accidental degeneracy remains at all pressures. Because of the high degree of anisotropy in the crystal, as evidenced by thermal expansion,[7] it would be surprising if the pressure-induced crystal field did not break this degeneracy, especially in the *Fmmm* orthorhombic phase. This is, in fact, predicted by our theory as shown by Fig. 6. Thus, regardless of the assumptions adopted, the explanation of experimental data is still not completely established.

Aside from the choice of unit cells, which only affects the interpretation of the dynamical properties, the only uncertainty in the calculation is in the repulsive part of the van der Waals potential U_V, and in the exchange energy $J(R)$. As mentioned earlier, recent measurements[12,13] indicate that $25\leq J\leq38$ K for the nearest-neighbor separation in α-O_2 at zero pressure, and its volume dependence has been unfolded from magnetic susceptibility data[13] only up to 6 kbar. There are also some *ab initio* results[14] for isolated O_2 pairs, but its accuracy and its applicability to the solid-phase magnetic interaction is not established. Similarly, the only information about the repulsive part of the van der Waals potential U_V comes from *ab initio* data[23] for the isolated O_2 pair and from unfolding molecular beam scattering data.[24] Not withstanding the inherent uncertainty in these results, it is well known that the effective pair potential in the solid is almost always considerably softer in the repulsive region than is appropriate for the isolated pair potential. Thus, the above-mentioned information can be regarded as no more than a guide. In this work we have fine tuned the potential used previously,[1] still well within the above-mentioned range of uncertainty, in an attempt to more accurately describe the properties of O_2 over a wide range of conditions. This has been largely successful. By incorporating the zero-point energy contributions directly into the optimization technique and carefully determining the minimum-energy structures for a wide range of pressures, a more detailed picture of the phase-transition region has emerged which clearly shows its first-order character. The fact that relatively small changes in the volume dependence of $J(R)$ and the repulsive part of U_V from previous work[1] has resulted in a change of the predicted orthorhombic transition pressure from 6 kbar previously to 24 ± 1 kbar shows how sensitive this transition is to the details of the potential. This sensitivity is a consequence of the delicate cancellation of the repulsive van der Waals forces with the attractive magnetic force along the **a** axis which gives rise to a shear force. Significant refinements of the theory beyond this will depend on further experimental and theoretical information about the details of the van der Waals and magnetic interaction in the solid at short ranges.

It is evident from the results that the technique of using a general, deformable unit cell in minimizing the Gibbs free energy with zero-point contributions is a powerful method for predicting phase transitions in solids and the resulting structural lattice parameters make possible accurate calculations of the dynamical features of these systems. Clearly, applications of this method to solid fluorine, CO, and other molecular solids is highly desirable.

ACKNOWLEDGMENTS

The authors would like to thank D. Hochheimer, V. Chandrasekharan, and H. Jodl for their useful comments and interest in this work and the Colorado Institute for Computational Studies for providing time on the Control Data Corporation Cyber-205 computer. This work was supported by the U.S. Department of Energy under Contract No. DE-AC02-84ER45050.

[1]A. Helmy, K. Kobashi, and R. D. Etters, J. Chem. Phys. **80**, 2782 (1984); **82**, 473(E) (1985).

[2]R. Meier, M. P. van Albada, and Ad Lagendijk, Phys. Rev. Lett. **52**, 1045 (1984).

[3]H. J. Jodl, F. Bolduan, and H. D. Hochheimer Phys. Rev. B **31**, 7376 (1985). H. D. Hochheimer, H. J. Jodl, W. Henkel, and F. Bolduan, Chem. Phys. Lett. **106**, 79 (1984).

[4]J. E. Cahill and G. Leroi, J. Chem. Phys. **51**, 97 (1969).

[5]K. Kobashi, M. L. Klein, and V. Chandrasekharan, J. Chem. Phys. **71**, 843 (1979); I. A. Burakhovitch, I. N. Krupskii, A. I. Prokhavatilov, Y. A. Freiman, and A. I. Erenburg, Pis'ma Zh. Eksp. Teor. Fiz. **25**, 37 (1977) [JETP Lett. **25**, 32 (1977)]; I. N. Krupskii, A. I. Prokhvatilov, Y. A. Freiman, and A. I. Erenburg, Fiz. Nizk. Temp. **5**, 271 (1979) [Sov. J. Low Temp. Phys. **5**, 130 (1979)]; R. D. Etters, A. A. Helmy, and K. Kobashi, Phys. Rev. B **28**, 2166 (1983).

[6]Ad Lagendijk, R. Meier, K. Kobashi, and R. D. Etters (unpublished).

[7]I. N. Krupskii, A. I. Prokhavatilov, Y. A. Freiman, and A. I. Erenburg, Fiz. Nizk. Temp. **5**, 271 (1979) [Sov. J. Low Temp. Phys. **5**, 130 (1979)].

[8]R. Ahlriches, R. Penco, and G. Scoles, Chem. Phys. **19**, 119 (1976); K. Tang and J. Toennies, J. Chem. Phys. **66**, 1496 (1977).

[9]R. D. Etters, A. A. Helmy, and K. Kobashi, Phys. Rev. B **28**, 2166 (1983).

[10]M. F. Collins, Proc. Phys. Soc. London **89**, 415 (1966); R. A. Alikhanov, Pis'ma Zh. Eksp. Teor. Fiz **5**, 430 (1967) [JETP Lett. **5**, 349 (1967)]; R. J. Meier and R. B. Helmholdt, Phys. Rev. B **29**, 1387 (1984); P. W. Stephens, R. J. Birgeneau, C. F. Majkrzak, and G. Shirane, *ibid.* **28**, 452 (1983).

[11]V. A. Slyusarev, Y. A. Freiman, and R. P. Yankelevich, Pis'ma Zh. Eksp. Teor. Fiz. **30**, 292 (1979) [Sov. J. Low Temp. Phys. **6**, 105 (1980)]; **7**, 265 (1981) [**7**, 265 (1981)]; G. C. DeFotis, Phys. Rev. B **23**, 4714 (1981); E. J. Wachtel and R. G. Wheeler, J. Appl. Phys. **42**, 1581 (1971).

[12]P. W. Stephens, R. J. Birgeneau, C. F. Majkrzak, and G. Shirane, Phys. Rev. B **28**, 452 (1983).

[13]R. J. Meier, C. J. Schinkel, and A. de Visser, J. Phys. C **15**, 1015 (1982).

[14]M. C. van Hemert, P. Wormer, and A. van der Avoird, Phys. Rev. Lett. **51**, 1167 (1983); R. Meier, Phys. Lett. **95A**, 115 (1983).

[15]G. Herzberg, *Spectra of Diatomic Molecules* (Van Nostrand Reinhold, New York, 1950).

[16]J. H. Dymond and E. B. Smith, *The Virial Coefficient of Gases* (Clarendon, Oxford, 1969).

[17]M. P. Orlova, Sov. J. Phys. Chem. **12**, 1603 (1966); W. F. Giaugne and H. L. Johnston, J. Am. Chem. Soc. **51**, 2300 (1929).

[18]R. Stevenson, J. Chem. Phys. **27**, 673 (1957).

[19]R. L. Mills, unpublished data.

[20]J. W. Stewart, J. Phys. Chem. Solids **12**, 122 (1959).

[21]D. Schiferl, D. Cromer, L. Schwalbe, and R. L. Mills, Acta Cryst. B **39**, 153 (1983).

[22]B. Olinger, R. L. Mills, and R. B. Root, J. Chem. Phys. **81**, 5068 (1984).

[23]A. van der Avoird (unpublished).

[24]V. B. Leonas, A. V. Sermyagin, and N. V. Kamyshov, Chem. Phys. Lett. **8**, 282 (1971).